

## First-principles calculation of the magnetocrystalline anisotropy energy of the pnictide MnSb

This article has been downloaded from IOPscience. Please scroll down to see the full text article.

1992 J. Phys.: Condens. Matter 4 10469

(<http://iopscience.iop.org/0953-8984/4/50/035>)

View [the table of contents for this issue](#), or go to the [journal homepage](#) for more

Download details:

IP Address: 171.66.16.159

The article was downloaded on 12/05/2010 at 12:44

Please note that [terms and conditions apply](#).

# First-principles calculation of the magnetocrystalline anisotropy energy of the pnictide MnSb

N Vast, B Siberchicot and P G Zerah

CEA Centre d'Etudes de Limeil-Valenton, 94195 Villeneuve-St-Georges Cédex, France

Received 23 June 1992, in final form 28 September 1992

**Abstract.** The magnetocrystalline anisotropy energy (MAE) of the pnictide MnSb is investigated by means of the augmented spherical wave method. The spin-orbit coupling enters the variational step of the procedure and the force theorem is applied to determine the dependence of the MAE on the directions of magnetization. Our numerical results agree well with the first-order development of anisotropy energy in uniaxial crystal structures. The easy axis of magnetization is then found to be in the basal plane of the hexagonal structure in agreement with experiment, and the first-order anisotropy constant is given.

## 1. Introduction

The magnetocrystalline anisotropy energy (MAE) is an important property of magnetic compounds and its calculation has been a long-standing problem. Since the first studies of Brooks [1] a large amount of work has been dedicated to the calculation of the MAE. Recently an investigation of the MAE for 3d metals (Fe, Co and Ni) was reported by Daalderop *et al* [2]. In that work, the spin-orbit coupling was included in the calculations to provide the anisotropy energy, and the many-body problem was treated with the linear-muffin-tin method in the framework of the local spin-density approximation (LSDA). Daalderop *et al* pointed out the difficulties encountered in the calculations when attempting to determine small energies (the MAE for Co is about  $60 \mu\text{eV}/\text{atom}$ ).

In this paper we present an augmented spherical wave (ASW) spin-polarized band-structure calculation, including spin-orbit coupling, of manganese pnictide MnSb whose MAE is determined by applying the so-called force theorem. This compound was chosen because of its large anisotropy energy ( $E_a = -210 \mu\text{eV}/\text{unit cell}$  corresponding to an anisotropy field  $H_a = 11 \text{ kOe}$ ).

## 2. Determination of the magnetocrystalline anisotropy energy by band-structure calculations

The internal energy of ferromagnetic materials depends on the direction of spontaneous magnetization. We consider here one part of this energy, the MAE,

which possesses the crystal symmetry of the material. For a material exhibiting uniaxial anisotropy, such as a hexagonal crystal, the MAE can be expressed as [3]

$$E(\theta) = K_1 \sin^2 \theta + K_2 \sin^4 \theta + K_3' \sin^6 \theta + K_3 \sin^6 \theta \cos[6(\varphi + \psi)] + \dots \quad (1)$$

where  $K_i$  is the anisotropy constant of the  $i$ th order,  $\theta$  and  $\varphi$  are the polar angles of the Cartesian coordinate system where the  $c$  axis coincides with the  $z$  axis (the Cartesian coordinate system was chosen such that the  $x$  axis is rotated through  $90^\circ$  from the  $a$  hexagonal axis) and  $\psi$  is a phase angle.

Both the dipolar interaction and the spin-orbit coupling give rise to the MAE, the former contributing only to the first-order constant  $K_1$ . In this paper, we deal with the MAE caused only by the spin-orbit interaction.

### 2.1. Ab-initio determination of the magnetocrystalline anisotropy energy

Following Jansen [4], the MAE is a ground-state property whose origin lies in the spin-orbit interaction (i.e. coupling between the spin of an independent particle and its own orbit) and can therefore be determined within the density-functional theory by an appropriate relativistic form of the effective single-particle equation of Kohn and Sham. The expression for the total ground-state energy of an  $N$ -electron system under spin-polarized formalism is [5, 6]

$$E_{\text{TOT}}^{\text{df}}(\tilde{n}, \mathbf{n}_1) = E_0(\mathbf{n}_1) - E_1(\tilde{n}, \mathbf{n}_1) \quad (2)$$

where  $E_0$  is the sum of one-particle eigenvalues (including core states):

$$E_0(\mathbf{n}_1) = \sum_{\alpha} \sum_{\substack{i=1 \\ \epsilon_{i\alpha} \leq E_F}}^N \epsilon_{i\alpha}$$

$$E_1[\tilde{n}, \mathbf{n}_1] = \int \int n(\mathbf{r}) v_{\text{el-el}}(\mathbf{r} - \mathbf{r}') n(\mathbf{r}') d^3 \mathbf{r}' d^3 \mathbf{r}$$

$$+ \sum_{\alpha\beta} \int v_{\alpha\beta}^{\mathbf{x}}(\mathbf{r}) \tilde{n}_{\beta\alpha}(\mathbf{r}) d^3 \mathbf{r} - E_{\mathbf{x}}[\tilde{n}]$$

where  $\alpha$  and  $\beta$  are the spin indices, and  $\tilde{n}$  is the two-by-two density matrix, whose elements are obtained from the one-electron eigenfunctions  $\psi_{\alpha i}(\mathbf{r})$ :

$$\tilde{n}_{\alpha\beta} = \sum_{i=1}^N \psi_{\alpha i}(\mathbf{r}) \psi_{\beta i}^*(\mathbf{r}).$$

The MAE between the two directions of magnetization is the change in total ground-state energy when aligning atomic moments along those directions:

$$E_a = E_{\text{TOT}}^{\text{df}}(\mathbf{n}_1) - E_{\text{TOT}}^{\text{df}}(\mathbf{n}_2) \quad (3)$$

where  $\mathbf{n}_1$  and  $\mathbf{n}_2$  are the directions between which the MAE is evaluated.

However, even in materials with a large anisotropy energy such as MnSb, this quantity is very small compared with the total ground-state energy (415 keV/unit cell), and sufficient numerical accuracy is difficult to attain. Instead of direct subtraction of the total ground-state energy, we used the so-called force theorem [2, 6], which states that, provided that the variation in the atomic moment direction can be treated as a perturbation keeping the unit-cell volume constant, the first-order change in total energy is given by the difference in the sum of eigenvalues calculated in each direction from the same self-consistently converged effective potential  $v_{\text{eff}}^{\text{sc}}(\mathbf{n}_1)$ :

$$E_{\mathbf{a}} = E_0(\mathbf{n}_2) - E_0(\mathbf{n}_1). \quad (4)$$

For valence electrons, the sum of single-particle eigenvalues is given by [6]

$$E_0^{\text{val}}(\mathbf{n}) = \int_{\epsilon_{\text{min}}}^{\epsilon_F(\mathbf{n})} \epsilon N(\mathbf{n}, \epsilon) d\epsilon \quad (5)$$

where  $N(\mathbf{n}, \epsilon)$  is the density of states (DOS) and  $\epsilon_{\text{min}}$  delimits the core and valence states.

Following Daalderop *et al* [2], we assume that the core-state contribution to the MAE is negligible and express it as

$$E_{\mathbf{a}} = \int_{\epsilon_{\text{min}}}^{\epsilon_F(\mathbf{n}_2)} \epsilon N(\mathbf{n}_2, \epsilon) d\epsilon - \int_{\epsilon_{\text{min}}}^{\epsilon_F(\mathbf{n}_1)} \epsilon N(\mathbf{n}_1, \epsilon) d\epsilon. \quad (6)$$

## 2.2. Details of the calculation

The electronic structure of MnSb was calculated using the ASW method of Williams *et al* [7]. The Dirac effective single-particle equation was approximated by the spin-polarized scalar-relativistic radial equation, including the Darwin and mass-velocity terms, but no spin-orbit term. Exchange and correlation were described in the LSDA.

The spin-orbit coupling operator was reintroduced into the Hamiltonian matrix at the variational step of the procedure. The spin-polarization and spin-orbit interactions were then treated simultaneously in the self-consistent loop.

MnSb crystallizes in the hexagonal NiAs structure (space-group,  $P6_3/mmc$ ) with two MnSb formulae per unit cell (figure 1). Antimony atom layers form a hexagonal close-packed structure (2a sites), whose octahedral sites are occupied by manganese atoms (2c sites) and tetrahedral sites are empty (4f sites). In the ASW ASA, atoms are represented by overlapping spheres, whose total volume must equal the unit-cell volume.

All calculations were performed with the 4.2 K experimental lattice constants given by Coehoorn *et al* [8] (table 1). The sphere radius ratio was arbitrarily chosen as the ASA radius ratio of Mn to Sb in their elementary solid states. No attempt was made to minimize the total ground-state energy by varying lattice parameters or by varying the radius ratio. However, when self-consistency was reached, the spin densities in the Mn and Sb atomic spheres were almost zero at the Wigner-Seitz radii, indicating that magnetic moment should be rather insensitive to the choice of sphere radii [9].

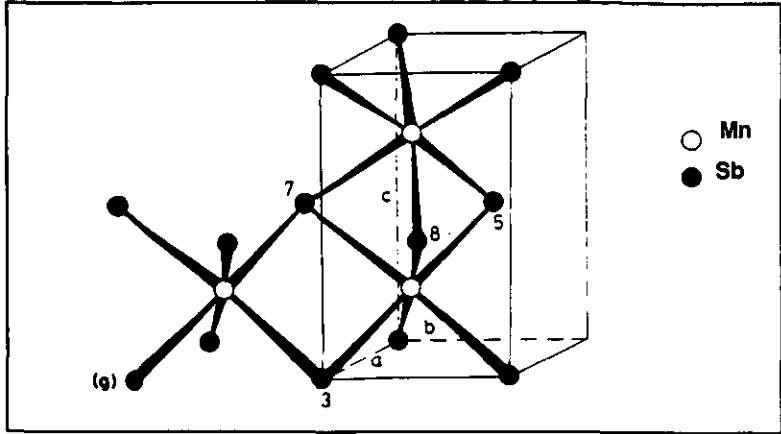


Figure 1. Ni-As-type hexagonal structure of MnSb [21].

Table 1. ASW input parameters.  $q_i$  is the number of sampling points in the irreducible Brillouin zone.  $\delta\epsilon$  is the energy-step mesh used for DOS sampling.

	$a$ (Å)	$R_{Mn}$ (Å)	$R_{Sb}$ (Å)	$R_{Sb}/R_{Mn}$	$c/a$	$q_i$	$\delta\epsilon$ (eV)
Our results	4.122	1.437	1.926	1.34	1.396	150 $k$ -points	0.136
Data from [8]	4.112	1.563	1.839	1.18	1.396	1000 $k$ -points	0.1

Self-consistency was considered to be reached when the difference between the sum of the eigenvalues of subsequent iterations was better than  $13.6 \mu\text{eV}/\text{unit cell}$  ( $\Delta E_0^{\text{val}} > E_a/15$ ). Other usual criteria, such as the charge density ( $\Delta Q > 10^{-5}e^-$ ) and magnetization ( $\Delta M > 10^{-3}\mu_B$ ) were more than satisfactory.

Band-structure calculations require the eigenvalue problem to be solved at selected  $k$ -points on a regular mesh in the Brillouin zone. To optimize computational efforts, lattice symmetries are used to reduce the initial set of  $k$ -points, each new  $k'$ -point of the reduced set being weighted according to symmetries [10]. However, as already pointed out by Coehoorn and de Groot [11], when taking spin-orbit coupling into account, the magnetic space group differs when changing the magnetic moment direction; therefore the number of  $k'$ -points in the reduced set differ when changing atomic moment directions. Calculations of the MAE  $E_a(\theta)$  (see equation (8)) were carried out keeping the same  $k$  mesh of the total Brillouin zone.

### 3. Results and discussion

#### 3.1. Spin-polarized calculations

The magnetic moments resulting from spin-polarized calculations without spin-orbit coupling are shown in table 2 and compared with both the previous ASW calculation of Coehoorn *et al* [8] and the experimental values of Bouwma *et al* [12]. The various input parameters are given in table 1.

Table 2. MnSb: theoretical spin magnetic moments and experimental value.

	Total magnetic moment ( $\mu_B$ per MnSb formula unit)	Mn site ( $\mu_B$ )	Sb site ( $\mu_B$ )
Our results	3.32	3.35	-0.032
Data from [8]	3.24	3.30	-0.06
Experimental data ( $T = 4.2$ K [12])	3.55		

Both theoretical calculations give similar results, although different Wigner-Seitz radius ratios were chosen. The exchange splitting is 3 eV and is calculated as the energy at the middle of the 3d majority band minus the energy at the middle of the 3d minority bands (Hankel energies in the ASW formalism [13]). The theoretical total magnetic moment is 6% lower than the experimental value.

### 3.2. Influence of spin-orbit coupling

An independent calculation including spin-orbit coupling was performed with the same input parameter and self-consistency criteria as in the former spin-polarized calculation in order to estimate the influence of spin-orbit interaction on the calculated properties. Atomic moments were kept parallel to the  $c$  axis.

(1) The total ground-state energy is lowered by 82 meV.

(2) The effects on the DOS are shown in figure 2 by subtraction of the calculated DOS with and without spin-orbit coupling. Both calculations were spin polarized, but the DOS is not shown spin projected. Deep valence states between -4.5 and -1.5 eV corresponding to Sb 5s states are marginally influenced by spin-orbit coupling. States between 1 eV and the Fermi level (7 eV) originate from overlapping Sb 5p and majority spin Mn 3d states.

(3) Exchange splitting is reduced by 22 meV. The spin contribution to the total magnetic moment is slightly reduced from  $3.32\mu_B$  to  $3.29\mu_B$  per formula unit and is mostly caused by the reduction in the number of excess majority spin electrons in Mn 3d states by 0.024 electrons. Such a reduction was also found by Min and Jang [14] for BCC and FCC iron.

### 3.3. Evaluation of the induced orbital moment

The part of the orbital moment induced by spin-orbit coupling was also calculated according to [15]. Taking this into account led to an increase in the total calculated moment by  $4.5 \times 10^{-2}\mu_B$  per formula unit. Nevertheless, this value does not account for the difference between the calculated and experimental magnetic moments.

As in Fe, Co and Ni systems [16], occupied spin-up electron states contribute negatively to the total orbital moment, whereas occupied spin-down electron states contribute positively.

The magnetomechanical factor was then estimated from [17]  $g' = (M_{\text{orb}} + M_{\text{spin}})/(M_{\text{orb}} + M_{\text{spin}}/2)$ , where  $M_{\text{spin}}$  is the spin contribution to the total magnetic moment and  $M_{\text{orb}}$  is the part of orbital moment induced by spin-orbit coupling. The magnetomechanical factor  $g'$  was found to be 1.973, in rather good agreement with the average experimental magnetomechanical factor  $g' = 1.978$  [18].

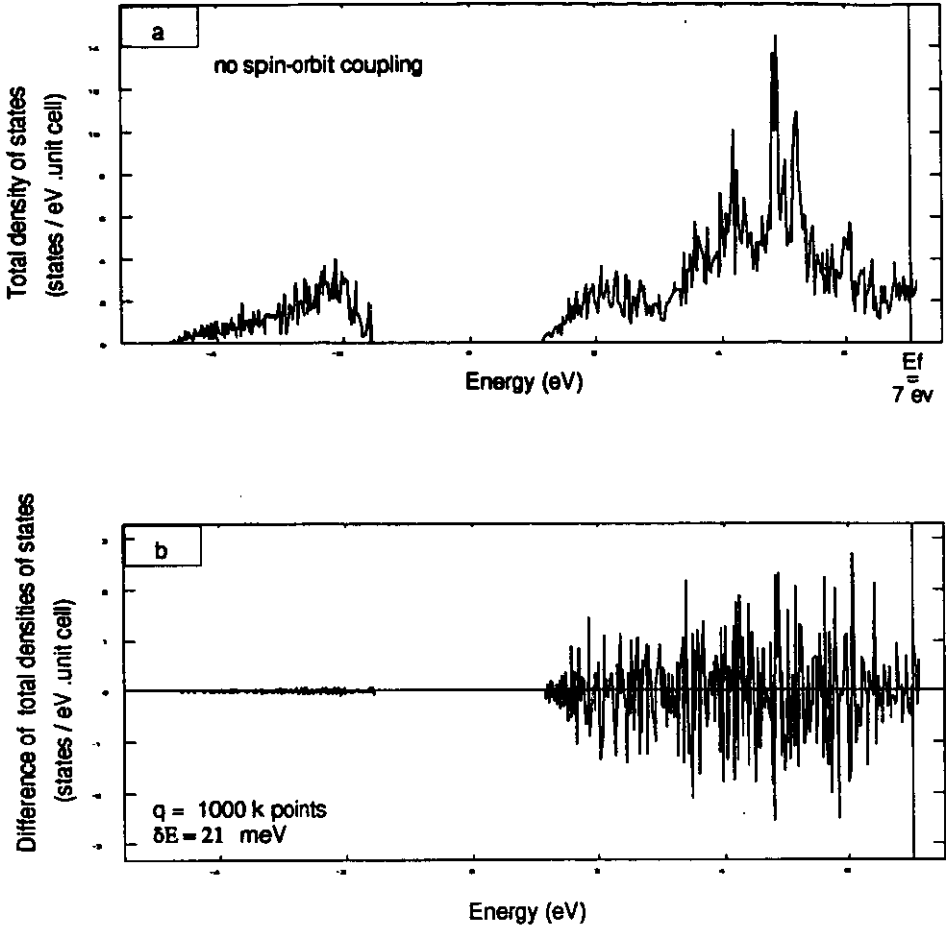


Figure 2. MnSb: influence of spin-orbit coupling on the total DOS: (a) total DOS within the scalar-relativistic approximation; (b) total DOS without spin-orbit coupling minus the total DOS with spin-orbit coupling.

### 3.4. The magnetocrystalline anisotropy energy

We then investigated the variation in the theoretical MAE with magnetization direction:

$$E_a(\theta_2, \varphi_2) = E_0^{\text{val}}(\theta_2, \varphi_2) - E_0^{\text{val}}(\theta_1, \varphi_1) \quad (7)$$

where  $(\theta_i, \varphi_i)$  are the  $n_i$  polar angles in the Cartesian coordinate system previously defined. As the dependence of the MAE on the azimuthal angle is a third-order term in equation (1), we set  $\varphi_i$  equal to zero in our calculations.

3.4.1. Variation in MAE with the angle  $\theta$  between the magnetization direction and the  $c$  axis. We first reached self-consistency by keeping the magnetic moments parallel to the  $c$  axis and applied the force theorem to several values of  $\theta$ :

$$E_a(\theta) = E_0^{\text{val}}(\theta) - E_0^{\text{val}}(0). \quad (8)$$

The calculated MAE  $E_a(\theta)$  is plotted in figure 3 for different meshes corresponding to  $q = 512, 1000, 1728, 4096$  and  $5832$   $k$ -sampling-points in the Brillouin zone. The numerical results (open squares) were fitted to the first-order development of equation (1) (full curves) giving the adjusted  $K_1$ -values summarized in table 3.

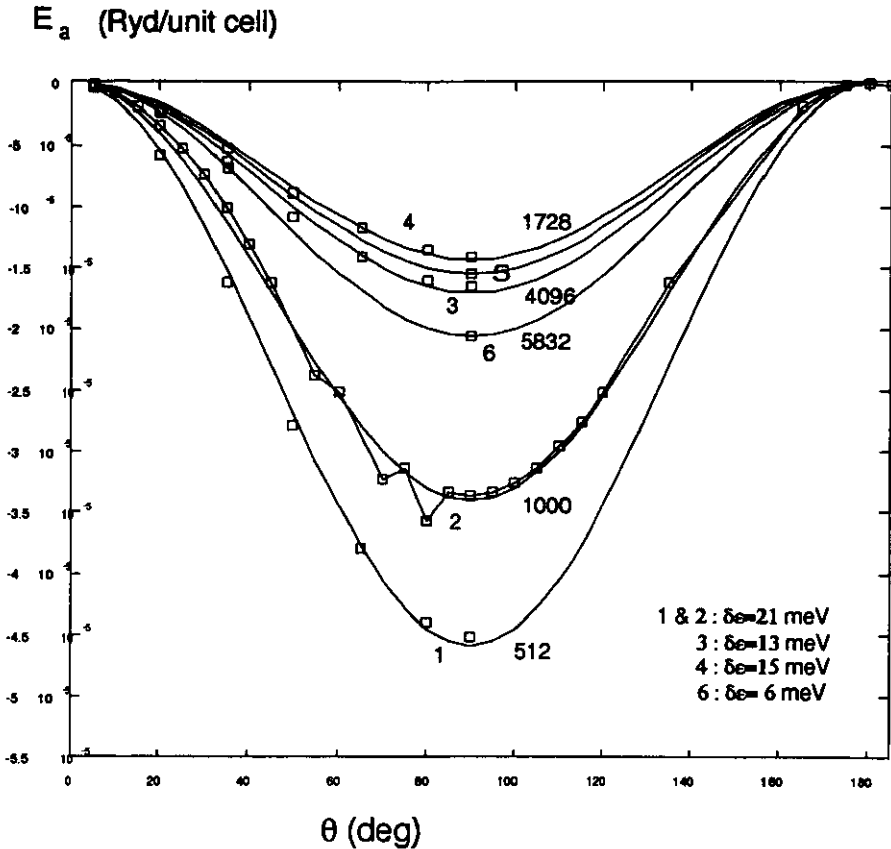


Figure 3. MnSb: variation in the MAE for different numbers of  $k$ -sampling-points in the Brillouin zone. Curve 5 is deduced from the experimental value [11].

Curve 5 is drawn with the value given by Coehoorn and de Groot [11]:  $E[100] - E[001] = -210$  meV/unit cell at 4.2 K.

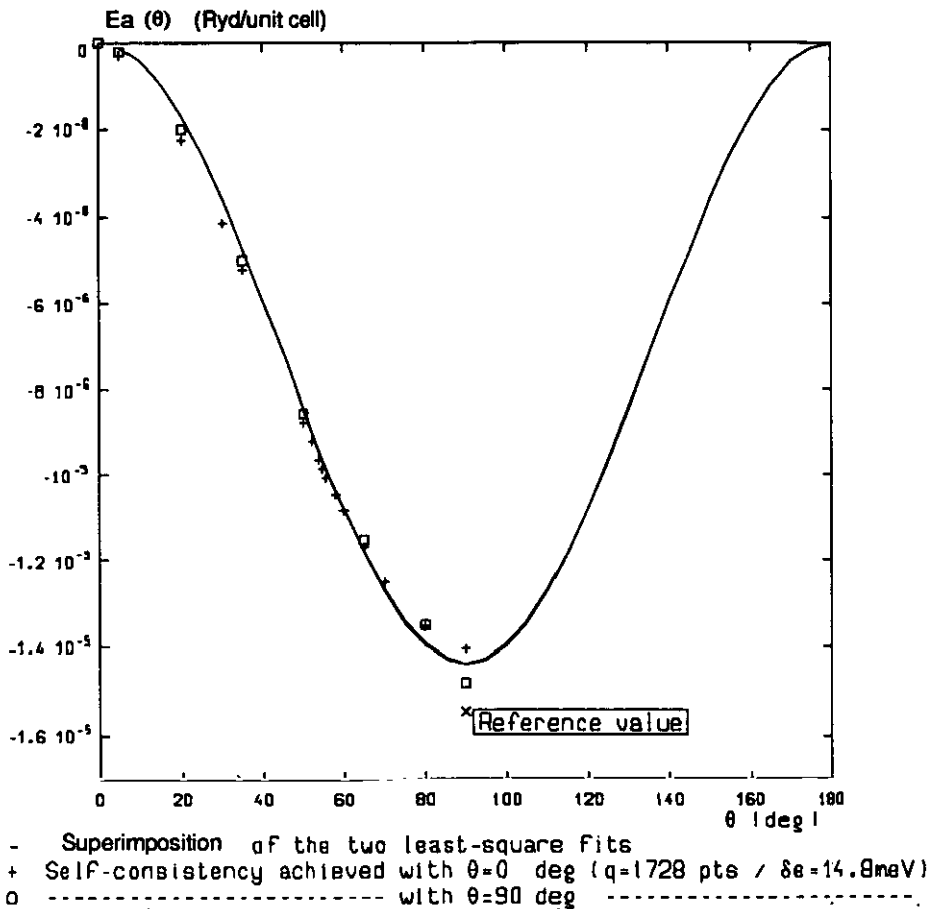
The calculated MAES agree well with the adjusted expression for uniaxial anisotropy. Curves 3, 4 and 6 seem to oscillate around the experimental value (curve 5). MAE minima are found at  $\theta = 90^\circ$ , giving experimental data according to which the magnetic moments lie in the basal plane of a hexagonal unit cell below the spin reorientation temperature (520 K) [19].

Attempts to fit the calculated MAES to a second-order model showed a small influence of the second-order anisotropy constant ( $K_2 \simeq K_1/10$ ) and agreement with the numerical results was neither improved nor made worse.



Table 3. MnSb: calculated first-order anisotropy constants  $K_1$ .

Curve (in figure 3)	$q$	$K_1$ (0 K) ( $J m^{-3}$ or $10 \text{ erg cm}^{-3}$ )	$K_1$ (0 K) ( $\mu\text{eV/unit cell}$ )
1	512	$-11.8 \times 10^5$	-624
2	1000	$-8.7 \times 10^5$	-462
3	1728	$-4.3 \times 10^5$	-230
4	4096	$-3.6 \times 10^5$	-193
6	5832	$-5.3 \times 10^5$	-281

Figure 4. MnSb: numerical and adjusted values of  $E_a(\theta)$  for two self-consistency directions.

The influence of the energy-step mesh  $\delta\epsilon$  used for DOS sampling was also checked for  $q = 1000$   $k$ -sampling-points in the Brillouin zone. Self-consistency was achieved at  $\theta = 0^\circ$  for  $\delta\epsilon = 45$  meV and  $\delta\epsilon = 136$  meV and the MAE was calculated with  $\theta = 90^\circ$ . We found an increase by 3% and 9%, respectively, related to calculation performed with  $\delta\epsilon = 21$  meV (curve 2).

**3.4.2. MAE dependence on self-consistency direction.** Further calculations were carried out to check the influence of the direction in which self-consistency is primarily reached on the calculated MAE. Self-consistency was now obtained keeping atomic

moments in the hexagonal basal plane. Brillouin zone sampling and the energy mesh were the same as those of curve 4 (figure 3), and the two results are compared. Figure 4 shows the superimposition of numerical and adjusted results of the two calculations. No difference was found in the first-order anisotropy constant value, and this is a further justification of the use of first-order force theorem.

#### 4. Conclusion

In this work, we have calculated the MAE in MnSb at low-temperature experimental volumes from first principles by applying the force theorem in the framework of the ASW formalism. Our numerical results agree well with first-order development of anisotropy energy in uniaxial crystal structures. The easy direction of magnetization was always found to be in the hexagonal basal plane, and the calculated value of the first-order anisotropy constant oscillates between  $-5.3 \times 10^5$  and  $-4.3 \times 10^5$  J m<sup>-3</sup> around the experimental value of  $-4 \times 10^5$  J m<sup>-3</sup>.

An attempt to go beyond the force theorem and to calculate the MAE by direct difference of total energies was unsuccessful, as we found it much more difficult to reach self-consistency in the total energy rather than in the sum of particle eigenvalues.

Application of this method to hexagonal bulk material is especially useful when no experimental data are available, such as for the hexagonal nitride Fe<sub>3</sub>N, whose easy axis of magnetization was determined [20]. Our next project is a general study and an *ab initio* evaluation of the MAE of barium hexaferrite BaFe<sub>12</sub>O<sub>19</sub>.

#### Acknowledgments

The authors are grateful to Dr S Matar (LCS CNRS, Bordeaux, France) and to Dr J Sticht (Technische Hochschule, Darmstadt, Germany) for fruitful discussions.

#### References

- [1] Brooks H 1940 *Phys. Rev.* **58** 909
- [2] Daalderop G H O, Kelly P J and Schuurmans M F H 1990 *Phys. Rev. B* **41** 11 919
- [3] Smith J and Wijn H P J 1959 *Ferrites* (Eindhoven: Philips Technical Library)
- [4] Jansen H J F 1990 *Magnetic Anisotropy (Science, Technology of Nanostructured Magnetic Materials)* ed G C Hadjipanayis and G A Prinz (New York: Plenum)
- [5] Von Barth U and Hedin L 1972 *J. Phys. C: Solid State Phys.* **5** 1629
- [6] Kubler J and Eyert V 1992 *Electronic Structure Calculations (Materials Science, and Technology)* ed K H Buschow (Weinheim: VCH Verlagsgesellschaft)
- [7] Williams A R, Kubler J and Gelatt C D Jr 1979 *Phys. Rev. B* **19** 6094
- [8] Coehoorn R, Haas C and de Groot R A 1985 *Phys. Rev. B* **31** 1980
- [9] Eriksson O, Norstrom L, Pohl A, Severin L, Boring A M and Johansson B 1990 *Phys. Rev. B* **41** 11 807
- [10] Monkhorst H J and Pack J D 1976 *Phys. Rev. B* **13** 5188
- [11] Coehoorn C and de Groot R A 1985 *J. Phys. F: Met. Phys.* **15** 2135
- [12] Bouwma J, van Bruggen C F, Haas C and van Laar B 1971 *J. Physique Coll.* **32** C1 78
- [13] Matar S 1992 *Z. Phys. B* **87** 91

- [14] Min B I and Jang Y R 1991 *J. Phys.: Condens. Matter* **3** 5131
- [15] Brooks M S S and Kelly P J 1983 *Phys. Rev. Lett.* **51** 1708
- [16] Eriksson O, Johansson B, Albers R C, Boring A M and Brooks M S S 1990 *Phys. Rev. B* **42** 2707
- [17] Singh M, Callaway J and Wang C S 1976 *Phys. Rev. B* **14** 1214
- [18] Scott G G 1961 *Phys. Rev.* **121** 104
- [19] *Gmelin Handbook of Inorganic Chemistry* 1983 (Berlin: Springer) system number 56 (manganese), part c, section 9
- [20] Siberchicot B, Vast N and Matar S 1992 *Proc. Int. Conf. on PTM* (Darmstadt: International Journal of Physics B) at press
- [21] West A R 1984 *Solid State Chemistry and its Applications* (New York: Wiley) ch 7